

Unusual metamagnetic transitions in $\text{Pr}_{0.5}\text{Ca}_{0.5}\text{Mn}_{0.97}\text{Ga}_{0.03}\text{O}_3$ studied by pulsed magnetic fields

Z. W. Ouyang, H. Nojiri, and S. Yoshii

Institute for Materials Research, Tohoku University, Sendai 980-8577, Japan

(Received 17 June 2008; published 9 September 2008)

Several unusual and intriguing magnetic phenomena have been observed in the Ga-doped manganite $\text{Pr}_{0.5}\text{Ca}_{0.5}\text{Mn}_{0.97}\text{Ga}_{0.03}\text{O}_3$. First, at 2.5 K, the magnetization steps and plateaus observed in the conventional $M(H)$ measurements with a sweep rate of less than 1 T/s are readily suppressed under an ultrafast magnetic field with a sweep rate of $\sim 10^3$ T/s. This feature is correlated with the collapse of the balance between the magnetic energy and the elastic energy within the martensiticlike scenario. Second, the zero-field cooled $M(H)$ curve consists of two metamagnetic features, which were not observed in the conventional low-field magnetization measurements and might be associated with the coexistence of the pseudo-CE-type and the CE-type antiferromagnetic phases. Third, both the antiferromagnetic and ferromagnetic phases may coexist under certain combinations of the magnetic field and temperature. The temperature-field phase diagram exhibits a minimum critical field for the antiferromagnetic to ferromagnetic transition. Similarities with other magnetic phase-separated systems are pointed out.

DOI: [10.1103/PhysRevB.78.104404](https://doi.org/10.1103/PhysRevB.78.104404)

PACS number(s): 75.30.Kz, 75.60.Ej, 75.47.Lx

I. INTRODUCTION

Phase separation phenomenon is a transformation of a homogeneous system in two or more phases and commonly encountered in many materials.^{1–5} In perovskite manganites, the phase separation is manifested by a coexistence between ferromagnetic (FM) metal phase and antiferromagnetic (AFM) insulator matrix. Competition between both phases strongly depends on magnetic field and temperature. An example is $\text{Pr}_{1-x}\text{Ca}_x\text{MnO}_3$, in which charge ordering phenomenon is robust around $x=0.5$, the “idea” ratio of $\text{Mn}^{3+}/\text{Mn}^{4+}$.^{6–8} The critical field to destroy the charge ordered (CO) state is much higher and reaches 25 T at very low temperature.⁷ Accordingly, the AFM insulator to FM metal transition is fully reversible, accompanying a large hysteresis. In order to weaken the CO state, one has to deviate the Mn^{4+} (hole) concentration from the nominal $x=0.5$. As a result, the CO AFM state can be melted into a FM metal state by a lower external magnetic field, thus pushing the AFM-FM transition boundary toward low fields. Meanwhile, an irreversible AFM-FM transition appears at low temperature, accompanying the appearance of a minimum critical field for the transition.^{6,7}

It is worth noting that the robust AFM CO ground state can also be suppressed by substitutions in the Mn site by a small amount of cations, such as Mg^{2+} , Sc^{3+} , Ga^{3+} , Fe^{3+} , etc.^{9–15} The resultant manganites $\text{Pr}_{1-x}\text{Ca}_x\text{Mn}_{1-y}M_y\text{O}_3$ (where $x \sim 0.5$, $y \sim 0.05$, and M is a magnetic or nonmagnetic cation) exhibit a phase-separated ground state, in which the disordering effect originating from the Mn-site substitution favors the development of FM domains within the AFM CO matrix. Thus, the critical field required to induce the AFM insulator to FM metal transition can be much reduced, facilitating the intensive study of this system. An important result is the observation of a succession of sharp steps separated by plateaus on the $M(H)$ curves below 10 K and 9 T. These magnetization steps are very sensitive to various parameters.^{11–15} For example, decreasing the field sweep rate can delay the magnetic instability, resulting in an upward

shift of the steps, even their disappearance.^{12,15} The observation of the magnetization jumps is understood within the martensiticlike scenario.^{12,15} Recent neutron-diffraction and synchrotron powder-diffraction experiments carried out on $\text{Pr}_{0.5}\text{Ca}_{0.5}\text{Mn}_{0.97}\text{Ga}_{0.03}\text{O}_3$ demonstrated two kinds of AFM phases: CE-type and pseudo-CE-type.^{16,17} It is the discontinuous collapse of the pseudo-CE-type AFM phase and the abrupt increase in the FM phase that lead to the observed steplike magnetization effects.¹⁶

Unlike the steplike plateaus, which are relatively well studied at low temperature ($T < 10$ K) and low field ($\mu_0 H < 9$ T) with low-field sweep rate ($dH/dT < 1$ T/s), the nature of the AFM insulator-FM metal transition is much less understood at high temperature and high field with much large field sweep rate. In this paper, we report the AFM-FM transition of $\text{Pr}_{0.5}\text{Ca}_{0.5}\text{Mn}_{0.97}\text{Ga}_{0.03}\text{O}_3$ under high fields up to 20 T and within a temperature range of 2.5–160 K. Owing to the application of ultrafast magnetic field, a different behavior is expected between our $M(H)$ curves and those obtained in a conventional magnetization measurement with a field sweep rate of less than 1 T/s. Since substituting Mn by 3% of Ga weakens the AFM CO state of $\text{Pr}_{0.5}\text{Ca}_{0.5}\text{MnO}_3$, one expects that the temperature dependence of the AFM-FM transition of $\text{Pr}_{0.5}\text{Ca}_{0.5}\text{Mn}_{0.97}\text{Ga}_{0.03}\text{O}_3$ resembles that of $\text{Pr}_{1-x}\text{Ca}_x\text{MnO}_3$ ($x < 0.5$). Similar evolution of the metamagnetic transition with temperature is expected to exist in other phase-separated systems.

II. EXPERIMENTAL DETAILS

The synthesis conditions of the ceramic sample $\text{Pr}_{0.5}\text{Ca}_{0.5}\text{Mn}_{0.97}\text{Ga}_{0.03}\text{O}_3$ were described in Ref. 16. Two bulk samples S1 and S2 were prepared from the same sample bar. The magnetization was measured by means of a standard inductive method. In each measurement, the sample was warmed up to 120 K, well above Curie temperature $T_C \sim 80$ K,¹³ to remove any residual FM state and then zero-field cooled (zfc) to the desired temperature. The pulsed magnetic fields were generated by a pulsed magnet driven by

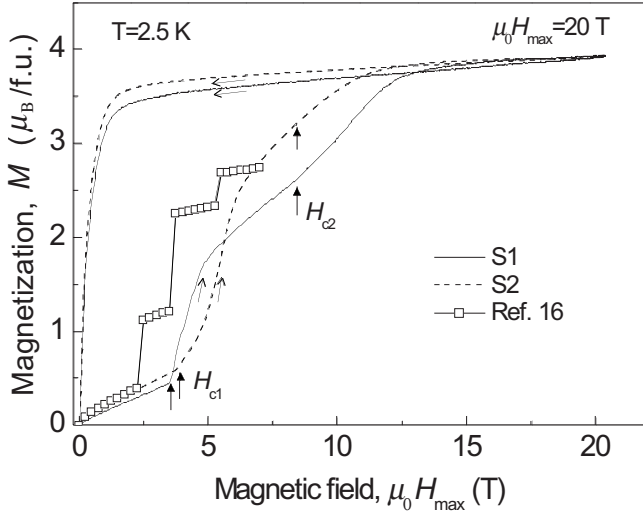


FIG. 1. The positive pulse zfc $M(H)$ curves of S1 and S2 measured at 2.5 K using pulsed field with $\mu_0 H_{\max} = 20$ T. The 2.5 K $M(H)$ curve in Ref. 16 is also shown for comparison. The thick arrows show the characteristic fields H_{c1} and H_{c2} for the metamagneticlike transitions. The thin arrows show the direction of the variation of the magnetic field.

a capacitor bank. To check the character of the AFM insulator-FM metal transition, we used pulsed fields of full sine shape, in which peak value $\mu_0 H_{\max}$ in the negative pulse is about 2/3 of that in the positive pulse (Ref. 18 for details). The magnetic-field sweep rate defined as $\mu_0 H_{\max} / t_{\max}$, where t_{\max} is the time taken for the field to reach $\mu_0 H_{\max}$, has a magnitude of 10^3 T/s, much larger than that achieved in a conventional magnetization measurement, which is usually smaller than 1 T/s.

III. EXPERIMENTAL RESULTS

A. Dynamic and thermal behaviors of the metamagnetic transitions

Figure 1 shows the positive pulse zfc $M(H)$ curves of S1 and S2 measured at 2.5 K using pulsed magnetic field with $\mu_0 H_{\max} = 20$ T (8×10^3 T/s). In this figure, the 2.5 K $M(H)$ curve of the bulk sample obtained in Ref. 16 is also presented for comparison. A common feature is that as the field increases, the low-field $M(H)$ curves exhibit nearly a linear increase, showing the AFM matrix of the compound. With further increase in the magnetic field, the magnetization increases rapidly and an AFM insulator to FM metal transition starts to be induced below 5 T, much lower than 25 T required for the parent compound $\text{Pr}_{0.5}\text{Ca}_{0.5}\text{MnO}_3$,⁷ indicating that the robust CO state in the parent compound is well suppressed by substituting Mn by 3% of Ga. The saturated magnetization of S1 and S2 is derived to be $M_s = 3.6 \mu_B/\text{f.u.}$, slightly larger than $3.4 \mu_B/\text{f.u.}$ of the Mn spin. Most importantly, Fig. 1 shows that the zfc $M(H)$ curve consisting of several sharp steps and plateaus in the conventional magnetization measurements (the average field sweep rate is not faster than 1 T/s)¹⁶ becomes quite smooth in the present measurements under an ultrafast magnetic field with a sweep rate of $\sim 10^3$ T/s.

Within the framework of martensiticlike scenario,^{11–15} the field induced AFM-FM metamagnetic transition is correlated with the competition between the magnetic energy favoring the formation of FM phase and the elastic energy related to elastic strains at the individual AFM/FM domain-wall interfaces, which tends to block the AFM-FM transition. For a low-field sweep rate (not faster than 1 T/s) applied in a conventional $M(H)$ measurement, a sudden magnetization jump is expected when the magnetic energy is large enough to overcome the elastic energy. The FM phase continues to grow rapidly until a balance between the magnetic energy and the increasing elastic energy is reached, thus resulting in a magnetization plateau. These two processes exist alternately in the H increasing branch, and the resulting $M(H)$ curve presents sharp steps separated by plateaus. For an ultrafast field sweep rate, the experimental time scale is much smaller than the character time for the balance between the magnetic energy and the elastic energy, and the system has no time to quickly respond to the excess magnetic energy. Within the extremely short experimental time, the driving force—the magnetic energy—remains larger than a certain threshold and the material overcomes a system-wide elastic energy barrier. Thus, the magnetization exhibits a continuous increase and a single flat plateau is not observed. In this sense, the smooth zfc $M(H)$ curves observed in the present study represent a nonequilibrium magnetization process. As a result of triggering the nonequilibrium magnetization process, the critical field required for the AFM-FM transition shifts to higher field (see below), as shown in Fig. 1.

Hardy and co-workers^{12,15} and Mahendiran *et al.*¹⁹ investigated the field spacing effects on the AFM-FM transition in Mn-site substituted manganites. In the measurements using a vibrating sample magnetometer where the magnetization data were recorded while sweeping the magnetic field (similar to the present measurements), a smaller field sweep rate can shift the magnetization step to higher field and cause the ultimate disappearance of the step, as was observed in the 3.25 K $M(H)$ curves of $\text{Pr}_{0.6}\text{Ca}_{0.4}\text{Mn}_{0.96}\text{Ga}_{0.04}\text{O}_3$.¹⁵ It was claimed that the disappearance of the magnetization step is correlated with the progressive accommodation of the martensitic strains when a very small field sweep rate is applied. We should note, however, that the $M(H)$ curve using a very small field sweep rate represents a near equilibrium magnetization process, different from the present measurement although both cases present similar smooth $M(H)$ curves. The result for the onset of near equilibrium is that the critical field for the onset of the AFM-FM transition shifts to low field.¹⁵

In addition to the global disappearance of the magnetization steps/plateaus caused by ultrafast magnetic field, Fig. 1 also shows that the smooth zfc $M(H)$ curve obtained in present measurements up to 20 T actually includes two metamagneticlike transitions—a rapid transition and a smooth one, whose shapes are sample dependent. For S1, the two metamagnetic transitions start at $\mu_0 H_{c1} = 3.5$ T and $\mu_0 H_{c2} = 8$ T, respectively. For S2, one rapid metamagnetic transition is observed at $\mu_0 H_{c1} = 4.0$ T, while the other one is quite confused but the anomaly around 8.0 T is indicative of its existence.

Figure 2 shows the zfc $M(H)$ curves of S1 measured at 2.5 K by varying the field sweep rate (i.e., by varying

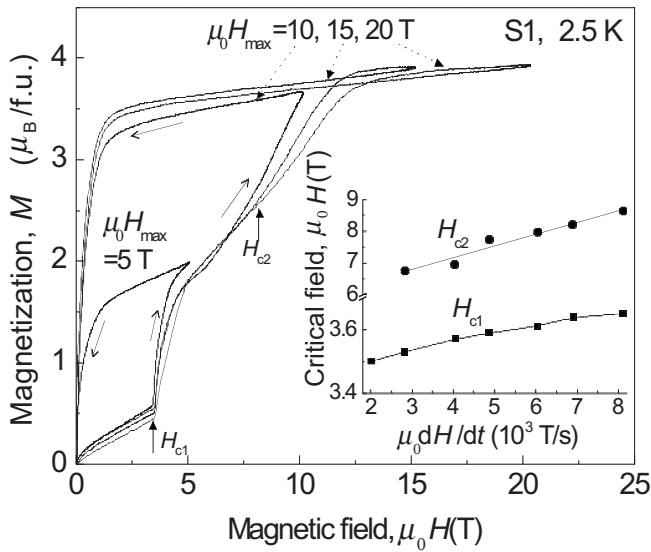


FIG. 2. The positive pulse zfc $M(H)$ curves of S1 measured at 2.5 K using pulsed fields with $\mu_0 H_{\max} = 5, 10, 15,$ and 20 T. The thick arrows show the characteristic fields H_{c1} and H_{c2} for the metamagneticlike transitions. The thin arrows show the direction of the variation of the magnetic field. The inset shows the H_{c1} and H_{c2} as a function of field sweep rate $\mu_0 dH/dt$.

$\mu_0 H_{\max}$). The two metamagneticlike anomalies are always observed for various sweep rates except for $\mu_0 H_{\max} = 5$ T, where the $M(H)$ curve exhibits a single sharp transition. By increasing the field sweep rate, H_{c1} and H_{c2} shift toward higher field accompanying the broadening of the transitions. This behavior is understood by considering the martensitic character of the AFM-FM transition. If the magnetization is measured in an ultrafast magnetic field, there is no time for the AFM matrix to nucleate and grow the new FM phase, thus moving H_{c1} and H_{c2} to higher fields (see the inset of Fig. 2). Dynamic behavior of the metamagnetic transition of $\text{Pr}_{0.5}\text{Ca}_{0.5}\text{Mn}_{0.97}\text{Ga}_{0.03}\text{O}_3$ is quite similar to another phase-separated system Gd_5Ge_4 .²⁰ We believe that the two-metamagnetic features in $\text{Pr}_{0.5}\text{Ca}_{0.5}\text{Mn}_{0.97}\text{Ga}_{0.03}\text{O}_3$ can be observed in a conventional magnetization measurement (see below) with low-field sweep rate. Thus, the two metamagnetic features show different dynamic behaviors from the steplike plateaus, which can be observed under a low-field sweep rate but tend to vanish under an ultrafast magnetic field.

Figure 3 shows the temperature dependence of the $M(H)$ curves of S1 measured using pulsed field with $\mu_0 H_{\max} = 15$ T as well as the 2.5 and 10 K zfc $M(H)$ curves obtained in the conventional measurement.¹⁶ The two metamagneticlike transitions observed at 2.5 K are still observed at temperature up to 140 K. Above 160 K, the two metamagnetic features vanish, which might point to the disappearance of the AFM ordering around this temperature recalling that the parent compound $\text{Pr}_{0.5}\text{Ca}_{0.5}\text{MnO}_3$ undergoes an AFM-paramagnetic (PM) transition at $T_N \sim 170$ K.^{6,7} In contrast, the magnetization steps and plateaus at 2.5 K zfc $M(H)$ curve are readily suppressed at 10 K (see also Ref. 16). These curves are far from saturation at 7 T and actually correspond to the first metamagneticlike transition of the present work if

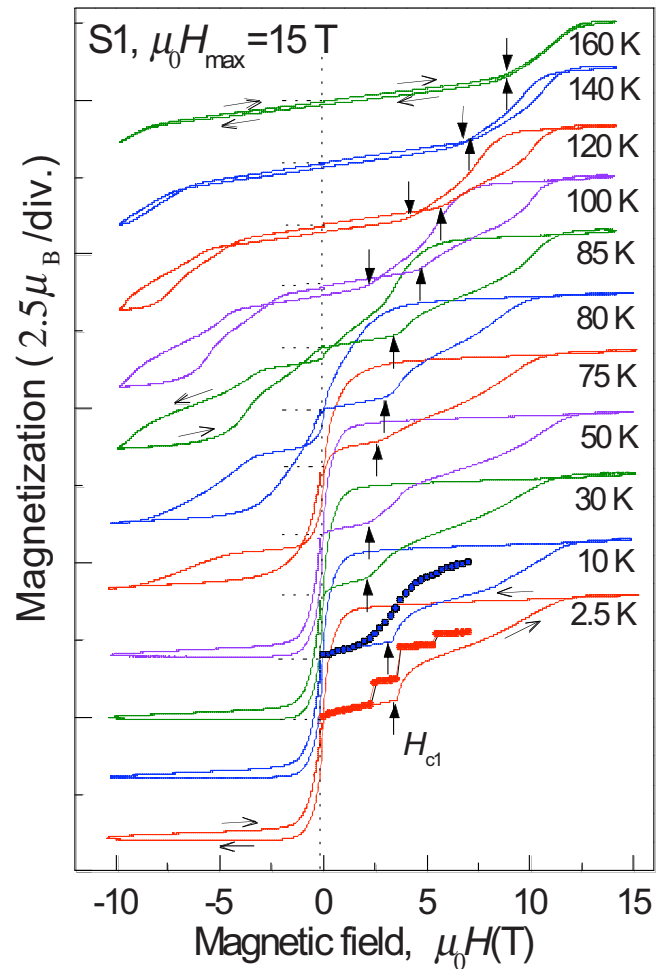


FIG. 3. (Color online) The full pulse zfc $M(H)$ curves of S1 measured at 2.5–160 K using pulsed field with $\mu_0 H_{\max} = 15$ T. The 2.5 and 10 K $M(H)$ curves in Ref. 16 are also shown for comparison. H_{c1} represents the onset of the metamagneticlike transitions in the zfc H -increasing process and the completion of the transition in the H -decreasing process for the positive pulse, which are shown by the thick arrows. The thin arrows show the direction of the variation of the magnetic field.

we ignore upward shift of the curve due to the influence of ultrafast field. It is very clear from Fig. 3 that the two metamagneticlike transitions observed in this study have a different thermal behavior from the steplike plateaus observed in Ref. 16.

Recently, the neutron-diffraction experiment up to 6 T showed that the magnetization steps/plateaus originate from the discontinuous pseudo-CE-type AFM-FM transition at ~ 3.5 T, but the CE-type AFM phase persists up to 5.5 T.¹⁶ This prompts us to assume that there is a higher character field responsible for the CE-type AFM-FM transition even in a conventional measurement. In other words, the formation of two metamagneticlike transitions is independent of field sweep rate and might be related to the competition between the CE-type and the pseudo-CE-type of AFM phases. At zero fields, the onset of CO state below $T_{\text{CO}} \sim 230$ K (Refs. 13 and 17) brings about lattice distortion in the AFM phase. The pseudo-CE-AFM phase is less distorted compared to the CE-

AFM phase¹⁷ and can be easily transformed into the FM metal phase with no or less lattice distortion, thus responsible for the first metamagnetic transition observed below ~ 7 T. The CE-type AFM-FM transition is responsible for the second metamagnetic transition between 7 and 13 T. The two metamagnetic features persist over a large temperature range (see Fig. 3) as long as the system is well in the AFM state but are rather sensitive to different samples (even from the same sample bar, see Fig. 1) in which the differences of the microstructures and the sample shape etc. may have a considerable influence on the shape of $M(H)$ curve. Note that in the polycrystalline samples of Hardy *et al.*, the 3.25 K zfc $M(H)$ curve of $\text{Pr}_{0.6}\text{Ca}_{0.4}\text{Mn}_{0.96}\text{Ga}_{0.04}\text{O}_3$ and the 2 K zfc $M(H)$ curve of Gd_5Ge_4 presented two metamagnetic features—a nearly discontinuous transition and a continuous one.¹⁵ The underlying physics is likely to be similar to the hypothesis proposed above. The hypothesis that the two-metamagnetic anomalies originate from two differently distorted AFM phases needs to be further confirmed by high-field x-ray or neutron-diffraction experiments of either $\text{Pr}_{0.5}\text{Ca}_{0.5}\text{Mn}_{0.97}\text{Ga}_{0.03}\text{O}_3$ or other phase-separated systems, e.g., Gd_5Ge_4 .

B. Interplay between reversible and irreversible metamagnetic phase transitions

Figures 1–3 illustrate that in the positive pulse, the low-temperature H -decreasing $M(H)$ curve deviates from the zfc H -increasing one, exhibiting a saturationlike curve until ~ 1 T where the magnetization drops rapidly and approaches zero at zero field. During the second increase in the magnetic field in the negative pulse, the magnetization curve presents similar shape as the demagnetization curve in the positive pulse (see Fig. 3), signaling that the field induced AFM-FM transition is fully irreversible, and once the FM phase is formed, it is stable at this temperature after removing the magnetic field.

Figure 3 also shows that the irreversible AFM-FM transition preserves until 50 K. For $T=75$ –85 K, however, the H -increasing $M(H)$ curves for the negative pulse exhibit a quite different shape as the H -decreasing curve in the positive pulse. A steplike FM behavior is seen in low fields. Hence, within this temperature range, the first application of field induces the FM phase in the entire AFM matrix. When the field is removed, a fraction of the sample volume is converted back into the AFM state (preferably the less distorted pseudo-CE-AFM phase), whereas the rest of the sample still remains in the FM state. That is, both the irreversible and reversible AFM-FM transformations coexist in this temperature range. Above ~ 85 K, the low-field $M(H)$ curves in the negative pulse no longer present a steplike FM phase. Thus, the AFM-FM transition becomes fully reversible above ~ 85 K. Note that above 160 K, the metamagnetic transition no longer exhibits any hysteresis and two-metamagnetic anomalies because around this temperature the AFM ordering disappears and the metamagnetic transition is a second-order PM-FM transition.

Defining H_{c1} as the field associated with the onset of the AFM-FM transition in the H -increasing process and the

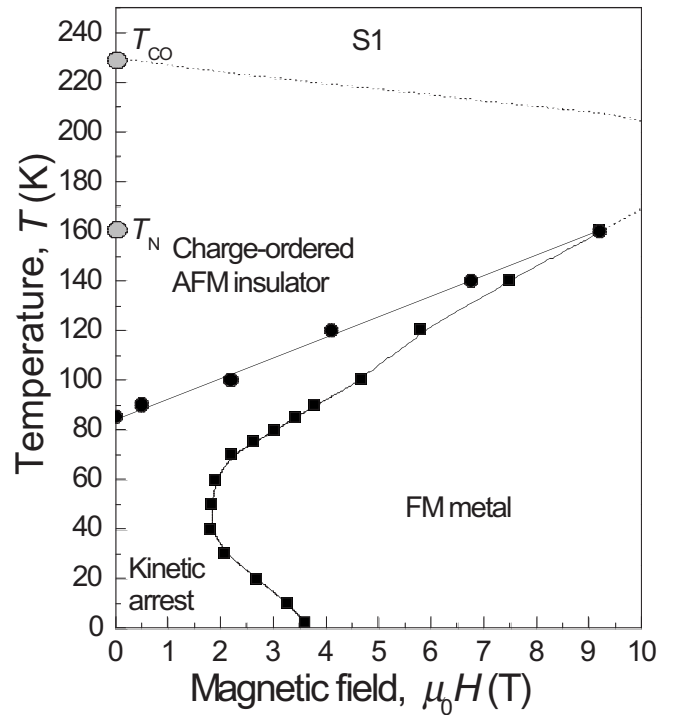


FIG. 4. The temperature-magnetic field phase diagram of S1 derived by plotting H_{c1} as a function of temperature (see also Fig. 3). A minimum H_{c1} is clearly seen within 40–60 K. The dotted lines are guides to the eyes. $T_{CO} \sim 230$ K is taken from Refs. 13 and 17.

completion of the FM-AFM transition in the H -decreasing process, we construct a temperature-field (T - H) phase diagram of S1 as shown in Fig. 4. It is very clear that compared to the T - H phase diagram of the parent compound $\text{Pr}_{0.5}\text{Ca}_{0.5}\text{MnO}_3$,⁷ the T - H phase diagram of the Ga-doped $\text{Pr}_{0.5}\text{Ca}_{0.5}\text{Mn}_{0.97}\text{Ga}_{0.03}\text{O}_3$ shifts the AFM-FM transition boundary toward low field. The value of H_{c1} decreases with increasing temperature ($dH_{c1}/dT < 0$), reaches a minimum at ~ 40 –60 K, and above this temperature, H_{c1} begins to increase with temperature ($dH_{c1}/dT > 0$). The minimum of H_{c1} between 40 and 60 K indicates that the compound is more easily converted into the FM state with field applied in this temperature range compared to the other ranges.

Based on the results presented above, substituting Mn by 3% of Ga in $\text{Pr}_{0.5}\text{Ca}_{0.5}\text{MnO}_3$ not only much reduces the critical field for the AFM-FM transition, which was well known from references, but also results in the observation of fully irreversible AFM-FM transition at low temperature, as well as the appearance of minimum critical field. This further confirms that substituting Mn by small amount of Ga plays a similar role in weakening the CO state as deviating the Mn^{4+} (hole) concentration from the idea $x=0.5$. Coexistence between the FM and AFM phases accompanying the appearance of a minimum critical field for the AFM-FM transition was also encountered in other phase-separated systems. For example, in magnetocaloric material Gd_5Ge_4 , a similar mix of reversibility and irreversibility of the AFM-FM transition was observed between ~ 10 and ~ 20 K. Within this temperature range, the critical field for the transition reaches minimum value.²¹

Recently, a phenomenological idea based on the concepts of supercooling and kinetic arrest was proposed to interpret the coexisting AFM and FM phases in Gd_5Ge_4 , the doped CeFe_2 and the oxide La-Pr-Ca-Mn-O .²² Based on this model, there are two regions in the phase diagram, i.e., the kinetic arrest region and the AFM-FM transition region. The low-temperature irreversibility of the AFM-FM transition is interpreted as kinetic arrest of the FM state, as shown in Fig. 4. This arrested FM state can be dearrested (or devitrificated) at high temperature. The minimum critical field is the result of intermix between the two regions in a complex way. After the sample is zfc, if the sample is magnetized at low temperature, one observes the dearrest of the metastable AFM phase, while at high temperature, one observes the AFM-FM transition. In the mediate temperature range, one observes the mixed behavior. When the AFM-FM phase transition boundary and the kinetic arrest boundary have opposite slopes, a minimal critical field is observed.

IV. CONCLUSIONS

In summary, the 2.5 K zfc $M(H)$ curve of $\text{Pr}_{0.5}\text{Ca}_{0.5}\text{Mn}_{0.97}\text{Ga}_{0.03}\text{O}_3$ containing several steps/plateaus in

the conventional measurement (less than 1 T/s) can become globally smooth if an ultrafast magnetic field with sweep rate of $\sim 10^3$ T/s is applied. Based on the martensiticlike scenario, it is the collapse of the balance between the magnetic energy and the elastic energy under an ultrafast field that results in the suppression of the magnetization steps. The zfc $M(H)$ curves measured up to 20 T present two distinct metamagnetic transitions having a different dynamic and thermal behavior from the metastable magnetization steps/plateaus. The two metamagnetic features might correspond to the pseudo-CE-type AFM to FM transition and the CE-type AFM to FM transition, respectively. The zfc compound exhibits a coexistence of the AFM and FM phases between ~ 70 and ~ 85 K. A minimum critical field for the AFM-FM transition is observed between ~ 40 and ~ 60 K, similar to other phase-separated systems, e.g., Gd_5Ge_4 .

ACKNOWLEDGMENTS

We thank C. Martin at Laboratory CRISMAT, France, for providing a sample of $\text{Pr}_{0.5}\text{Ca}_{0.5}\text{Mn}_{0.97}\text{Ga}_{0.03}\text{O}_3$ and for a very helpful discussion. This work was supported by Japan Society for the Promotion of Science.

-
- ¹S. B. Roy, G. K. Perkins, M. K. Chattopadhyay, A. K. Nigam, K. J. S. Sokhey, P. Chaddah, A. D. Caplin, and L. F. Cohen, *Phys. Rev. Lett.* **92**, 147203 (2004).
- ²Z. W. Ouyang, V. K. Pecharsky, K. A. Gschneidner, Jr., D. L. Schlager, and T. A. Lograsso, *Phys. Rev. B* **76**, 134406 (2007).
- ³P. A. Sharma, S. B. Kim, T. Y. Koo, S. Guha, and S.-W. Cheong, *Phys. Rev. B* **71**, 224416 (2005).
- ⁴M. Uehara, S. Mori, C. H. Chen, and S.-W. Cheong, *Nature (London)* **399**, 560 (1999).
- ⁵K. Sengupta and E. V. Sampathkumaran, *Phys. Rev. B* **73**, 020406(R) (2006).
- ⁶Y. Tomioka, A. Asamitsu, H. Kuwahara, Y. Moritomo, and Y. Tokura, *Phys. Rev. B* **53**, R1689 (1996).
- ⁷M. Tokunaga, N. Miura, Y. Tomioka, and Y. Tokura, *Phys. Rev. B* **57**, 5259 (1998).
- ⁸Y. Okimoto, Y. Tomioka, Y. Onose, Y. Otsuka, and Y. Tokura, *Phys. Rev. B* **57**, R9377 (1998).
- ⁹S. Hébert, A. Maignan, V. Hardy, C. Martin, M. Hervieu, and B. Raveau, *Solid State Commun.* **122**, 335 (2002).
- ¹⁰S. Hébert, V. Hardy, A. Maignan, R. Mahendiran, M. Hervieu, C. Martin, and B. Raveau, *J. Solid State Chem.* **165**, 6 (2002).
- ¹¹A. Maignan, S. Hébert, V. Hardy, C. Martin, M. Hervieu, and B. Raveau, *J. Phys.: Condens. Matter* **14**, 11809 (2002).
- ¹²V. Hardy, S. Hébert, A. Maignan, C. Martin, M. Hervieu, and B. Raveau, *J. Magn. Magn. Mater.* **264**, 183 (2003).
- ¹³A. Maignan, V. Hardy, C. Martin, S. Hébert, and B. Raveau, *J. Appl. Phys.* **93**, 7361 (2003).
- ¹⁴V. Hardy, C. Yaicle, S. Hébert, A. Maignan, C. Martin, M. Hervieu, and B. Raveau, *J. Appl. Phys.* **94**, 5316 (2003).
- ¹⁵V. Hardy, S. Majumdar, S. Crowe, M. R. Lees, D. McK. Paul, L. Hervé, A. Maignan, S. Hébert, C. Martin, C. Yaicle, M. Hervieu, and B. Raveau, *Phys. Rev. B* **69**, 020407(R) (2004).
- ¹⁶C. Yaicle, C. Martin, Z. Jirak, F. Fauth, G. André, E. Suard, A. Maignan, V. Hardy, R. Retoux, M. Hervieu, S. Hébert, B. Raveau, Ch. Simon, D. Saurel, A. Brûlet, and F. Bourée, *Phys. Rev. B* **68**, 224412 (2003).
- ¹⁷C. Yaicle, F. Fauth, C. Martin, R. Retoux, Z. Jirak, M. Hervieu, B. Raveau, and A. Maignan, *J. Solid State Chem.* **178**, 1652 (2005).
- ¹⁸H. Nojiri, K.-Y. Choi, and N. Kitamura, *J. Magn. Magn. Mater.* **310**, 1468 (2007).
- ¹⁹R. Mahendiran, A. Maignan, S. Hébert, C. Martin, M. Hervieu, B. Raveau, J. F. Mitchell, and P. Schiffer, *Phys. Rev. Lett.* **89**, 286602 (2002).
- ²⁰Z. W. Ouyang, H. Nojiri, S. Yoshii, G. H. Rao, Y. C. Wang, V. K. Pecharsky, and K. A. Gschneidner, Jr., *Phys. Rev. B* **77**, 184426 (2008).
- ²¹H. Tang, V. K. Pecharsky, K. A. Gschneidner, Jr., and A. O. Pecharsky, *Phys. Rev. B* **69**, 064410 (2004).
- ²²K. Kumar, A. K. Pramanik, A. Banerjee, P. Chaddah, S. B. Roy, S. Park, C. L. Zhang, and S.-W. Cheong, *Phys. Rev. B* **73**, 184435 (2006).